Supplementary Materials

Strongly Acidic SSZ-13 Zeolite Boosts High-Space-Velocity CO_2-to-Light Olefins Conversion via Synergistic Bifunctional Catalysis

Xiangzeng Chen[ac], Jiejie Ling[ac], Yan Gao[ac], Ming-Ao Sun[ac], Jilong Wang[b], Le Xu*[ac]

[a] *State Key Laboratory of Materials-Oriented Chemical Engineering, College of Chemical Engineering, Nanjing Tech University, Nanjing 211816, China.*

[b] *State Key Laboratory of Petroleum Molecular and Process Engineering, Shanghai Key Laboratory of Green Chemistry and Chemical Processes, School of Chemistry and Molecular Engineering, East China Normal University, Shanghai 200062, China.*

[c] *Suzhou Laboratory, Suzhou 215100, China.*

E-mail: lexu@njtech.edu.cn (L. Xu)

Experimental Section

Materials

Zirconium nitrate pentahydrate ($Zr(NO_3)_4 \cdot 5H_2O$, 99%), iron nitrate nonahydrate ($Fe(NO_3)_3 \cdot 9H_2O$, 99.99%), cerium nitrate hexahydrate ($Ce(NO_3)_3 \cdot 6H_2O$, 99.99%), gallium nitrate ($Ga(NO_3)_3$, 99.9%) and aluminum nitrate nonahydrate ($Al(NO_3)_3 \cdot 9H_2O$, 99%) were supplied by Macklin Co., Ltd. Colloidal silica (Ludox AS-40, 40 wt.% suspension in H_2O) was purchased from Sigma Aldrich. Zinc nitrate hexahydrate ($Zn(NO_3)_2 \cdot 6H_2O$, 99%), chromic nitrate nonahydrate ($Cr(NO_3)_3 \cdot 9H_2O$, 99.99%), D-(+)-Glucose (99.7%) and citric acid (99.5%) were purchased from Sinopharm Chemical Reagent Co., Ltd. Sodium hydroxide (NaOH, 96%) was purchased from Xilong Chemical Co., Ltd. Ammonium carbonate ($(NH_4)_2CO_3$, 99%) and aluminum isopropoxide ($Al(O\text{-}i\text{-}Pr)_3$, 99%) were purchased from Shanghai Adamas Reagent Co., Ltd. N,N,N-Trimethyl-1-ammonium adamantane (TMAdaOH, 25%) was purchased from Shanghai Haohong Bio-pharmaceutical Technology Co., Ltd. All chemicals were analytical grade and did not require further purification for use.

Synthesis of metal oxides

The metal oxide catalysts were synthesized predominantly by co-precipitation and sol-gel methods. The $ZnZrO_x$(a) solid solution catalyst was taken as a typical example of the co-precipitation method to describe the synthesis procedures, where a represents the molar ratio of Zn/(Zn+Zr) for the synthesis.[1] The total moles of metal ions are 0.0155 mol. A certain amount zinc nitrate hexahydrate ($Zn(NO_3)_2 \cdot 6H_2O$), zirconium nitrate pentahydrate ($Zr(NO_3)_4 \cdot 5H_2O$), or a mixture of $Zn(NO_3)_2 \cdot 6H_2O$ and zirconium $Zr(NO_3)_4 \cdot 5H_2O$ with a designed Zn/Zr molar ratio were first dissolved in 100 mL water at 70 °C. Then, 100 mL of aqueous solution containing 3.06 g ammonium carbonate ($(NH_4)_2CO_3$) was added to the aforementioned solution (at a flow rate of 3 ml min^{-1}) under vigorous stirring at 70 °C to form a precipitate. The suspension was continuously stirred for 2 h at 70 °C, followed by cooling down to room temperature, filtering, and washing three times with deionized water. The recovered sample was dried at 110 °C

overnight and calcined at 500 °C in air for 3 h. The same preparation technique was used for $GaZnZrO_x$ with a Ga : Zn : Zr molar ratio of 33 : 2.5 : 67 and $ZnZrAlO_x$ with a Zn : Zr : Al molar ratio of 13 : 87 : 5.

The $ZnFeZrO_x$ with Zn : Fe : Zr molar ratio of 0.13 : 0.05 : 0.87 was taken as a typical example of the sol-gel method to describe the synthesis procedure. $Zn(NO_3)_2 \cdot 6H_2O$, $Fe(NO_3)_3 \cdot 9H_2O$, and $Zr(NO_3)_4 \cdot 5H_2O$ were dissolved in the deionized water. Subsequently, a certain amount of citric acid (metal ions to actric acid molar ratio of 0.5) was added. Then, the mixture solution was stirred and heated to 80 °C to produce a highly viscous gel. The filtered sample was dried at 110 °C overnight and calcined at 500 °C in air for 3 h. The same preparation technique was used or Cr_2O_3, $GaZrO_x$ with a Ga : Zr molar ratio of 1 : 2 and $ZnCeZrO_x$ with a Zn : Ce : Zr molar ratio of 0.5 : 0.2 : 1.8 according to previous reports.[2-4]

Hydrothermal synthesis of aluminosilicate SSZ-13

The aluminosilicate SSZ-13 zeolite with CHA topology was synthesized by the hydrothermal synthesis method according to reported procedures.[5] A synthesis molar ratio of 1.0 SiO_2 : X Al_2O_3 : 0.25 TMAdaOH : 0.125 Na_2O : 44 H_2O was used, where X = 0.100, 0.050, 0.033 and 0.017 for Si/Al = 5, 10, 15 and 30, respectively. A typical synthesis involved adding 6.9630 g N,N,N-Trimethyl-1-ammonium adamantane (TMAdaOH) solution to 17.9438 g of deionized H_2O with stirring. Next, a desirable amount of aluminum isopropoxide ($Al(O\text{-}i\text{-}Pr)_3$) and NaOH was added to the aqueous TMAdaOH solution and the mixture was stirred under ambient conditions for 15 min. Finally, 4.9500 g of colloidal silica (Ludox AS-40) was added to the mixture and stirred for 2 h under ambient conditions. The synthesis solution was then transferred to a 50 mL Teflon-lined stainless-steel autoclave (Anhui Chem-n Instrument Co., Ltd.) and placed in a forced convection oven at 160 ºC and rotated at 20 rpm for 8 d. The crystalline zeolite solid was recovered by three cycles of centrifugation and washing with DI water. The recovered product was dried at 80 ºC for 12 h. Finally, the sample was calcined at 550 °C for 6 h to remove the organic template. The resulting sample

was labeled as SSZ-13(x), where x represents the Si/Al ratio in the gel.

Hydrothermal synthesis of other zeolites.

SAPO-34 (CHA topology), ZK-5 (KFI topology), LTA (LTA topology), ERI (ERI topology) and RHO (RHO topology) zeolites were synthesized according to the reported procedure.[6-9]

SAPO-34 zeolite was prepared with the synthetic gel containing colloidal silica (JN-40), pseudo-boehmite (Al_2O_3), tetraethylammonium hydroxide (TEAOH), phosphoric acid (H_3PO_4) and deionized water. The mixture was stirred for 2 h to form homogeneous gel with a composition of 0.3 SiO_2 : 1.0 Al_2O_3 : 2.0 TEAOH : 1.0 P_2O_5 : 70 H_2O. The synthesis solution was then transferred to a Teflon-lined stainless steel autoclave at 200 ℃ for 2 d.

ZK-5 zeolite was synthesized with the colloidal silica (Ludox AS-40), potassium hydroxide (KOH), Aluminum hydroxide ($Al(NO_3)_3$), 18-crown-6, strontium nitrate ($Sr(NO_3)_2$) and deionized water. The mixture was stirred at room temperature for 30 min. The obtained gel had a composition of 0.23 K_2O : 0.1 Al_2O_3 : 1.0 SiO_2 : 0.1 18-crown-6 : 0.01 SrO : 16 H_2O. The synthesis solution was then transferred to a Teflon-lined stainless steel autoclave and allowed to crystallize at 150 ℃ for 5 d.

LTA-type zeolite was synthesized with tetraethylorthosilicate (TEOS), HF, aluminum hydroxide ($Al(OH)_3 \cdot H_2O$), tetramethylammonium hydroxide pentahydrate ($TMAOH \cdot 5H_2O$), and deionized water. The mixture was stirred for 24 h at room temperature with a composition of 0.50 ROH : 0.05 TMAOH : 0.49 HF : 1.0 SiO_2 : 0.025 Al_2O_3 : 5.0 H_2O, where R is the imidazolium-based OSDA. The synthesis solution was then transferred to a Teflon-lined stainless steel autoclave and allowed to crystallized at 175 ℃ for 3 d.

RHO-type zeolite was synthesized with colloidal silica (Ludox AS-40), sodium aluminate ($NaAlO_2$), sodium fluoride (NaF), RHO zeolite seeds, alkali metal-crown ether (AMCE-2) complex and deionized water. The mixture was stirred for 24 h at room temperature in terms of a composition of 0.04 Na_2O : 0.04 Al_2O_3 : 1.0 SiO_2 : 0.02 NaF

: 0.16 (AMCE-2 complex) : 6.4 H_2O. The synthesis solution was then transferred to a Teflon-lined stainless steel autoclave and allowed to crystallize at 140 ℃ for 6 d.

ERI-type zeolite was synthesized with colloidal silica (Ludox AS-40), aluminium sec-butoxide ($Al[OCH(CH_3)C_2H_5]_3$), tetrapropylammonium hydroxide (TPAOH) hexamethonium bromide (TCI), and potassium hydroxide solution (KOH). The composition of the initial reactant mixture was as follows: 6.37 TPAOH : 1.63 RBr_2: 0.72 K_2O : 0.8 Al_2O_3 : 16 SiO_2 : 258 H_2O, where RBr_2 represents hexamethonium bromide. The initial reactant mixture was finally transferred to an autoclave for hydrothermal treatment at 150 °C for 5 d.

All the recovered products were dried at 80 °C for 12 h. Finally, the samples were calcined at 550 °C for 6 h to remove the organic template. The resulting sample was labeled as zeolite(x), where x represents the Si/Al ratio in the gel.

Ion-exchange of the calcined zeolites to produce the proton-type zeolite

The calcined zeolite was treated with 0.5 mol L^{-1} NH_4Cl solution (solid-to-liquid ratio of 1 g : 100 mL) at 65 °C for 3 h for twice. The sample was washed several times with deionized water and then calcined at 550 °C for 6 h. The final samples obtained were labeled as H-zeolite(x).

Synthesis of OXZEO bifunctional catalysts

The bifunctional tandem catalysts were fabricated through a mechanochemical blending protocol combining metal oxides with zeolite components. In a standard procedure, metal oxide and zeolite were homogenized at a 2:1 (mass ratio) grinding for 10 min. The resulting composite mixture underwent sequential processing: uniaxial pressing at 10 MPa, and size fractionation to 20 - 40 mesh particles. All preparations maintained strict stoichiometric control unless explicitly modified for comparative studies.

CO_2 hydrogenation to methanol

The catalytic reaction of CO_2 hydrogenation to methanol was evaluated using a high-pressure tubular fixed-bed reactor, and the products were detected by an on-line gas chromatograph (FULI 80) equipped with a thermal conductivity detector (TCD) and two flame ionization detectors (FID). Typically, the $ZnZrO_x$(a) solid solution (0.12 g) was first pretreated in Ar flow (30 mL min^{-1}) at 400 °C and atmospheric pressure for 2 h. Then the CO_2 and H_2 mixture with a CO_2/H_2 ratio of 1/3 (with 4 vol% N_2 as internal standard) was introduced in the reactor at 320 °C, 4 MPa and GHSV of 21,000 mL g_{cat}^{-1} h^{-1}. The selectivity of hydrocarbon products was calculated on a molar carbon basis. The selectivity of CO was calculated separately. All the data discussed in this work was collected after 12 h of reaction for CO_2 hydrogenation reaction. TCD and TDX-01 packed column connections (1 m × 1/8 inch), FID connected with HP-PLOT AL2O3S capillary column (30 m × 0.53 mm × 15μm), using Ar (99.999%) as carrier gas. H_2, CO_2, N_2, CO are analyzed by TCD, hydrocarbon products are analyzed by FID 1, and oxygenated hydrocarbons such as CH_3OH are analyzed by another FID 2. Almost no hydrocarbons were detected in FID 1. CO_2 conversion (X), and product selectivity (S) were calculated using the following equations:

$$X(CO_2) = \frac{CO_{out} + CH_3OH_{out}}{CO_{2out} + CO_{out} + CH_3OH_{out}} \times 100\% \quad (1)$$

$$S(Product) = \frac{Product_{out}}{CO_{out} + CH_3OH_{out}} \times 100\% \quad (2)$$

where CO_{2out}, CO_{out} and CH_3OH_{out} are the outlet amounts (moles) of CO_2, CO, and CH_3OH respectively.

Supplementary Figures

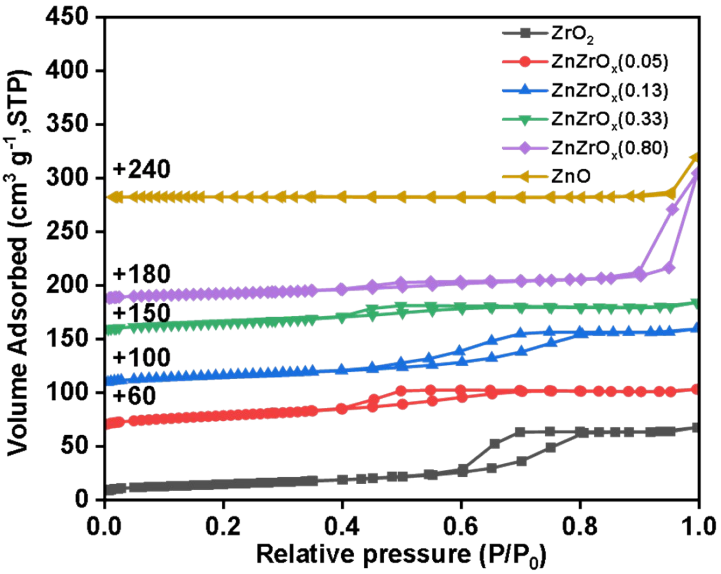

Fig. S1 N_2 adsorption-desorption isotherms profiles of ZrO_2, ZnO and $ZnZrO_x$(a) oxides with different Zn/(Zn+Zr) molar ratios.

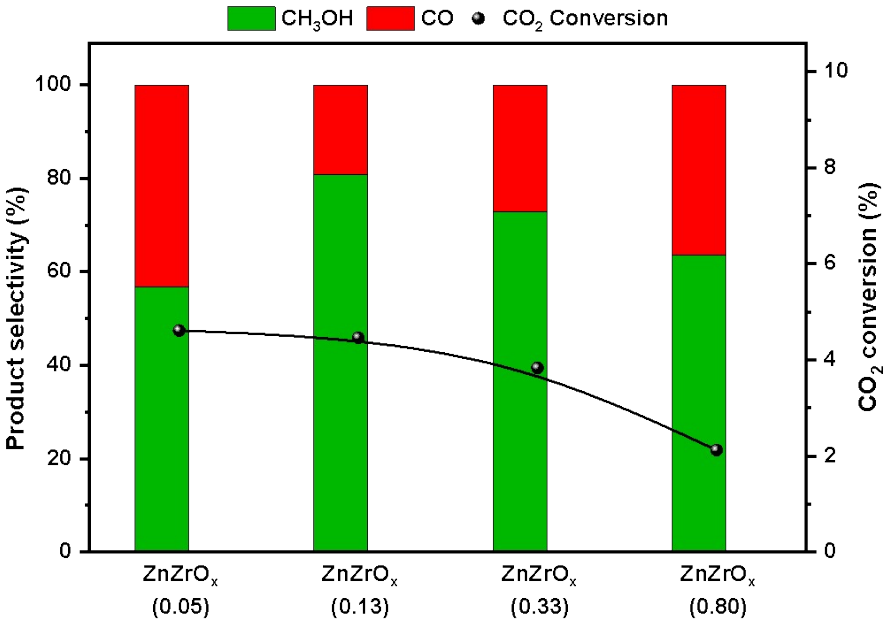

Fig. S2 Catalytic performance of CO_2 hydrogenation to methanol. CO_2 conversion and product distribution obtained over $ZnZrO_x$(a) oxide (reaction conditions: H_2/CO_2 = 3:1, GHSV = 21,000 mL g_{cat}^{-1} h^{-1}, 4 MPa and 320 ºC).

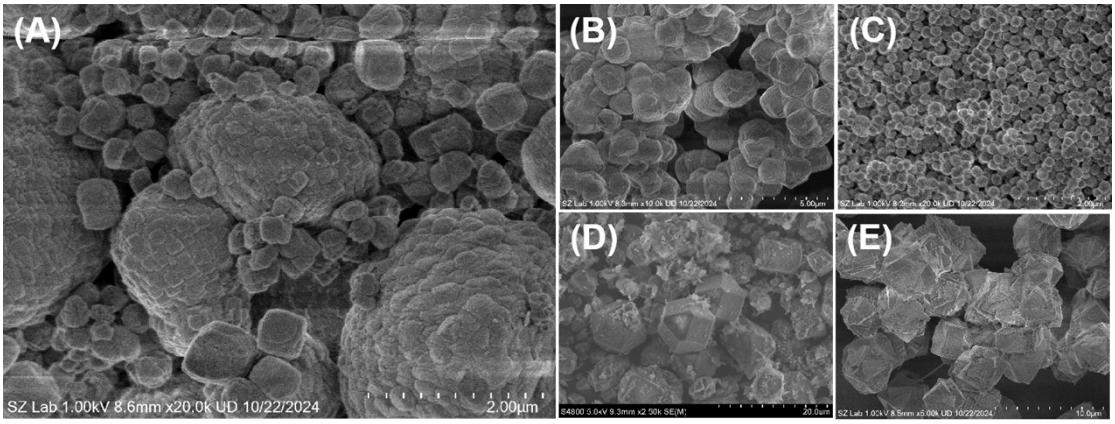

Fig. S3 SEM images of (A) H-SSZ-13(30), (B) H-RHO(12.5), (C) H-ERI(10), (D) H-LTA(20) and (E) H-ZK-5(5) zeolite.

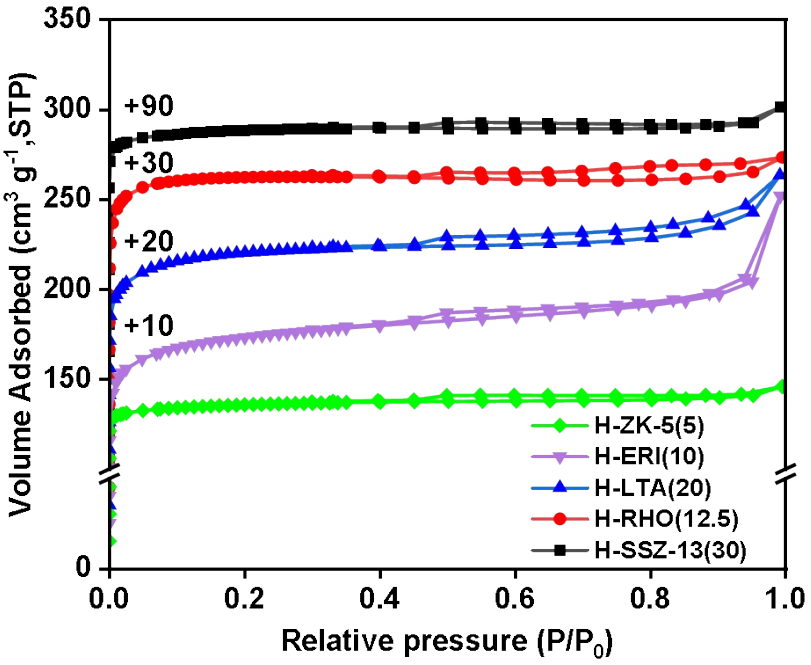

Fig. S4 N_2 adsorption-desorption isotherms profiles of H-ZK-5(5), H-ERI(10), H-LTA(20), H-RHO(12.5) and H-SSZ-13(30) zeolite.

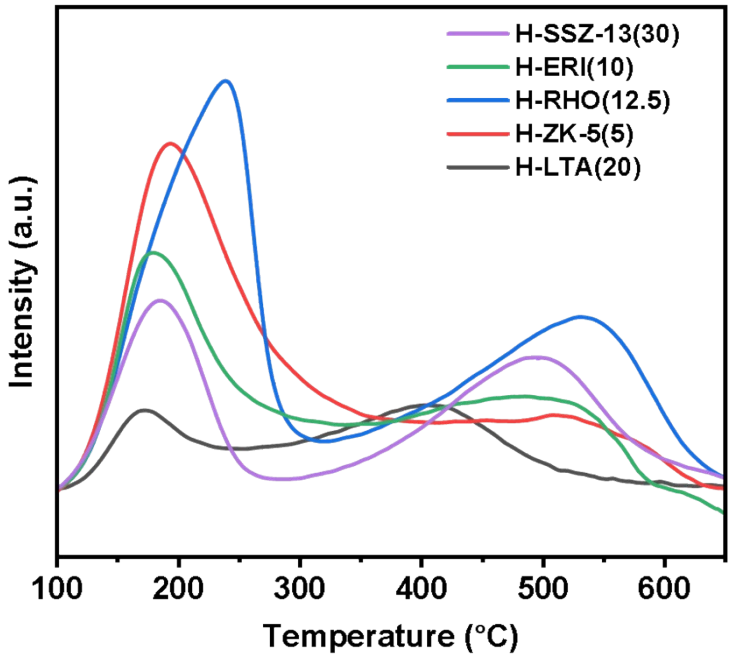

Fig. S5 NH_3-TPD pattern of H-ZK-5(5), H-ERI(10), H-LTA(20), H-RHO(12.5), and H-SSZ-13(30) zeolite.

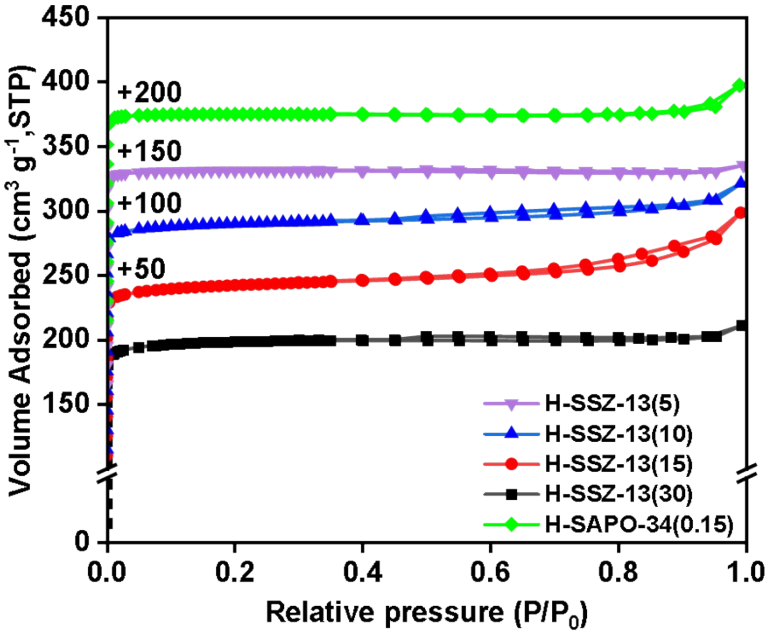

Fig. S6 N_2 adsorption-desorption isotherms profiles of H-SAPO-34(0.15), H-SSZ-13(5), H-SSZ-13(10), H-SSZ-13(15) and H-SSZ-13(30) zeolite.

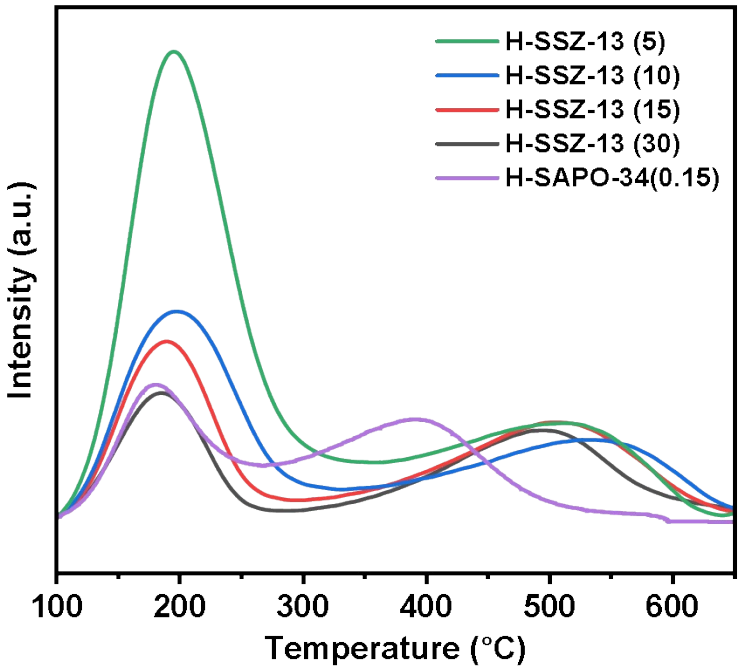

Fig. S7 NH_3-TPD pattern of H-SAPO-34(0.15), H-SSZ-13(5), H-SSZ-13(10), H-SSZ-13(15) and H-SSZ-13(30) zeolites.

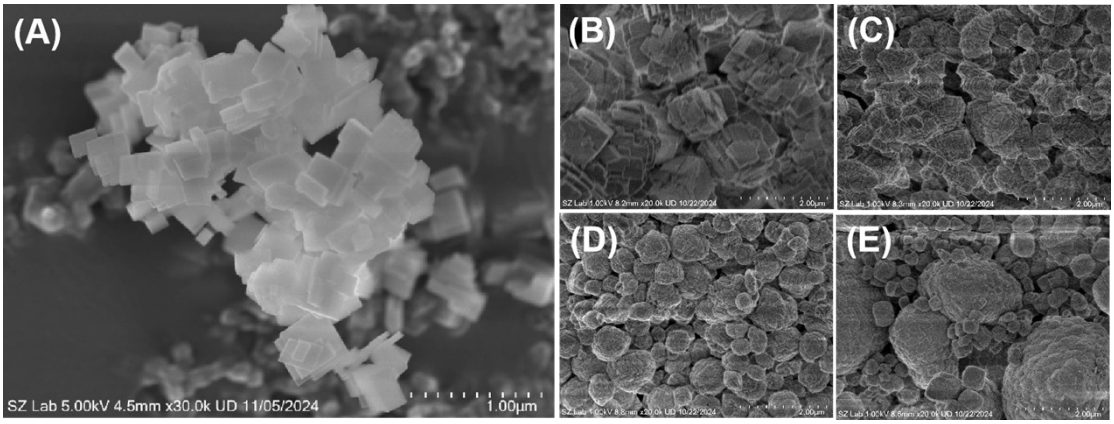

Fig. S8 SEM images of (A) H-SAPO-34(0.15), (B) H-SSZ-13(5), (C) H-SSZ-13(10), (D) H-SSZ-13(15) and (E) H-SSZ-13(30) zeolite.

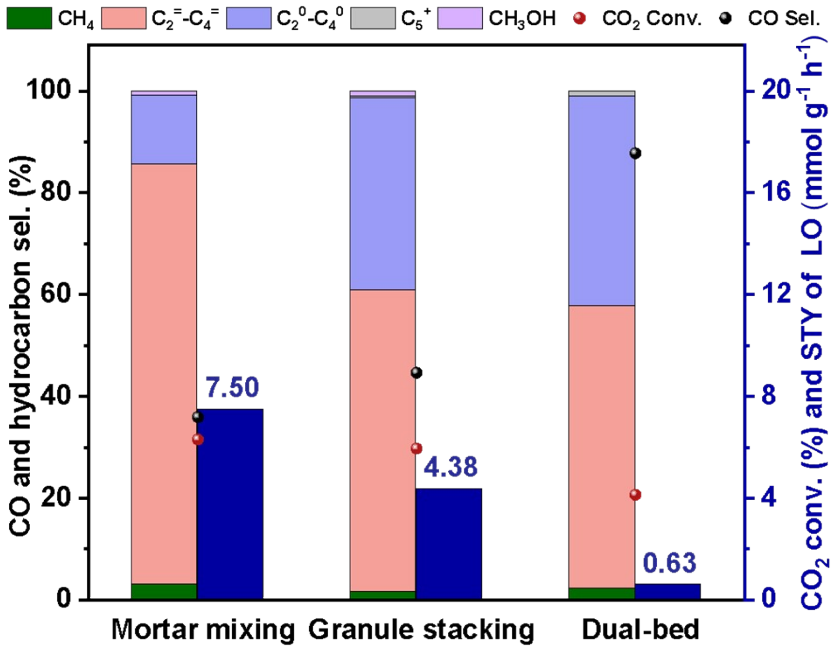

Fig. S9 Catalytic performance of CO_2 hydrogenation into light olefins. Effect of mix mode of oxide and zeolite components on the catalytic performance of $ZnZrO_x(0.13)$ oxide and H-SSZ-13(30) zeolite (reaction conditions: H_2/CO_2 = 3:1, GHSV = 21,000 mL g_{cat}^{-1} h^{-1}, 1 MPa and 380 ºC). LO: light olefins.

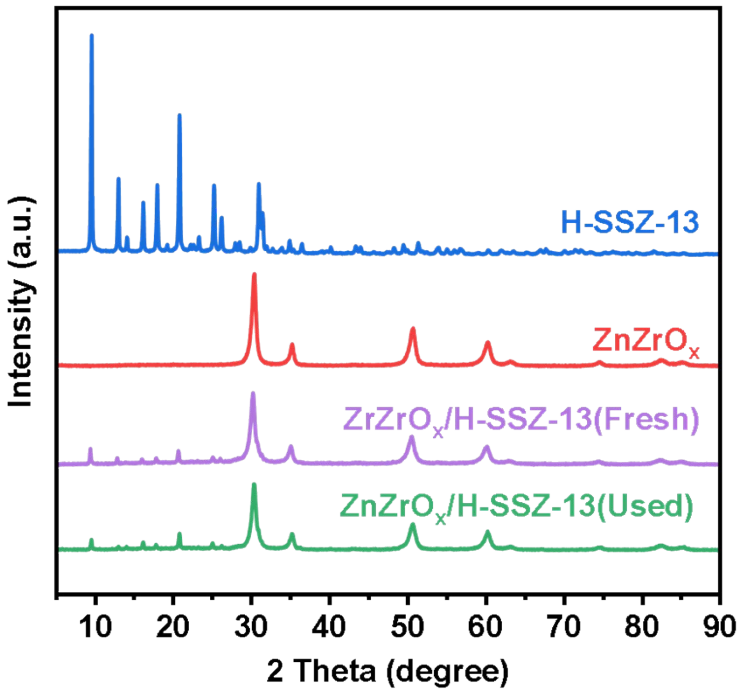

Fig. S10 PXRD patterns of $ZnZrO_x$(0.13), H-SZZ-13(30), $ZnZrO_x$/H-SSZ-13(fresh), and $ZnZrO_x$/H-SSZ-13(used).

Supplementary Tables

Table S1. Physical and chemical properties of $Zn_aZr_{1-a}O_x$.

Sample	Zn/(Zn+Zr)[a]	S_{total}[b] ($m^2\ g^{-1}$)	PV_{total}[e] ($cm^3\ g^{-1}$)	Amount of desorbed CO_2 ($\mu mol\ g^{-1}$)
ZrO_2	0	51.2	0.10	178.0
$ZnZrO_x(0.05)$	4.5%	67.3	0.07	240.0
$ZnZrO_x(0.13)$	11.2%	56.8	0.09	191.9
$ZnZrO_x(0.33)$	29.5%	54.0	0.05	151.4
$ZnZrO_x(0.80)$	83.0%	43.4	0.19	153.5
ZnO	1	7.0	0.06	23.1

[a] The Zn/(Zn+Zr) ratios of samples were measured by XRF.

[b] Calculated by BET plot.

[c] Calculated based on P/P_0 = 0.99.

Table S2. Surface area and pore volume properties of various zeolites.

Sample	S_{total}[a] ($m^2\ g^{-1}$)	S_{inter}[c] ($m^2\ g^{-1}$)	S_{exter}[b] ($m^2\ g^{-1}$)	PV_{total}[d] ($cm^3\ g^{-1}$)	PV_{micro}[b] ($cm^3\ g^{-1}$)	PV_{meso}[e] ($cm^3\ g^{-1}$)
H-ERI(10)	505.3	389.4	115.9	0.37	0.20	0.17
H-LTA(20)	612.4	528.3	84.1	0.38	0.27	0.10
H-ZK-5(5)	428.3	396.5	31.8	0.23	0.20	0.03
H-RHO(12.5)	699.5	670.2	29.3	0.38	0.35	0.03
H-SAPO-34(0.15)	504.8	496.5	8.3	0.37	0.26	0.11
H-SSZ-13(5)	526.5	518.7	7.8	0.29	0.28	0.01
H-SSZ-13(10)	550.8	509.9	40.9	0.34	0.28	0.07
H-SSZ-13(15)	560.2	505.5	54.7	0.38	0.27	0.11
H-SSZ-13(30)	574.0	539.2	34.8	0.33	0.29	0.04

[a] Calculated by BET plot.

[b] Calculated by *t*-plot.

[c] S: surface area, $S_{inter} = S_{total} - S_{exter}$.

[d] Calculated based on $P/P_0 = 0.99$.

[e] PV: pore volume, $PV_{meso} = PV_{total} - PV_{micro}$.

Table S3. Chemical composition and acidity properties of various zeolites.

Sample	Si/Al[a]	Amount of desorbed NH_3 (mmol g^{-1})			
		Total	Weak	Medium	Strong
H-ERI(10)	6.0	1.25	0.44 (183 ºC)	0.41 (286 ºC)	0.40 (479 ºC)
H-LTA(20)	18.5	0.52	0.09 (174 ºC)	0.30 (330 ºC)	0.13 (416 ºC)
H-ZK-5(5)	3.5	1.35	0.51 (190 ºC)	0.43 (255 ºC)	0.41 (464 ºC)
H-RHO(12.5)	8.0	1.81	1.02 (220 ºC)	0.29 (420 ºC)	0.50 (535 ºC)
H-SAPO-34(0.15)	0.18	1.16	0.48 (180 ºC)	0.68 (390 ºC)	/
H-SSZ-13(5)	4.2	1.69	1.04 (198 ºC)	0.38 (345 ºC)	0.27 (517 ºC)
H-SSZ-13(10)	7.0	1.40	0.76 (198 ºC)	0.33 (406 ºC)	0.31 (540 ºC)
H-SSZ-13(15)	9.7	1.24	0.56 (189 ºC)	0.27 (414 ºC)	0.41 (517 ºC)
H-SSZ-13(30)	16.6	0.91	0.38 (185 ºC)	0.05 (366 ºC)	0.48 (490 ºC)

[a] Si/Al ratios were measured by XRF.

Table S4. Comparison of the catalytic performance between our catalyst and the other reported catalysts.

Sample	Temp. (°C)	Pressure (MPa)	O/Z	H_2/CO_2	GHSV (mL g_{cat}^{-1} h^{-1})	CO_2 conv.	CO sel.	$C_2^=$-$C_4^=$ sel.	Yield (%)	STY (mmol g_{cat}^{-1} h^{-1})	Ref.
Cr_2O_3/H-SAPO-34	370	0.5	0.5	3	4,000	12.7	36.0	95.8	7.79	3.34	1
$ZnGa_2O_4$/H-SAPO-34	400	3	0.5	3	5,400	22.0	66.0	80.0	5.98	3.46	10
$Zn_{0.5}Ce_{0.2}Zr_{1.8}O_4$ /H-RUB-13(200)	350	3.5	1	3	4,800	22.1	34.5	72.2	10.45	5.37	11
	350	3.5	1	6	4,800	30.1	26.5	72.7	16.08	4.73	
	350	3.5	1	3	9,600	7.86	26.4	77.19	4.46	4.59	
$ZnZrO_x$/Zn-SAPO-34	380	2	2	3	3,600	12.0	65.0	80.0	3.36	1.30	12
	380	2	2	3	15,000	6.52	36.32	90.0	3.59	6.01	
	380	2	2	3	20,000	5.65	33.16	92.5	3.49	7.49	
$GaZrO_x$/H-SAPO-34	390	3	0.5	3	3,000	26.7	52.4	88.8	11.28	3.63	13
	390	3	0.5	3	4,500	23.3	53.8	90.2	9.70	4.68	
	390	3	0.5	3	6,000	21.4	53.0	90.9	9.12	5.86	
In−Zr/H-SAPO-34	400	3	2	3	9,000	35.5	85	76.7	4.08	3.94	14
	400	3	2	3	13,500	31.5	81.7	80.4	4.63	6.70	
	400	3	2	3	15,750	29.0	78.2	83.9	5.30	8.95	
$ZnFeAlO_4$/H-SAPO-34	380	4	1	4	4,000	42.0	50.0	83.0	17.43	5.98	15
	380	4	1	6	4,000	48.5	48.0	80.0	20.18	4.94	

Sample	Temp. (°C)	Pressure (MPa)	M/Z	H_2/CO_2	GHSV (mL g_{cat}^{-1} h^{-1})	CO_2 conv.	CO sel.	$C_2^=$-$C_4^=$ sel.	Yield (%)	STY (mmol g_{cat}^{-1} h^{-1})	Ref.
$ZnAl_2O_4$/H-SAPO-34	370	3	0.5	3	5,400	15.0	49.0	87.0	6.66	3.85	16
$ZnZrO_x$/H-SSZ-13(10)	380	1	2	3	21,000	6.34	35.0	86.48	3.56	8.02	This work
$ZnZrO_x$/H-SSZ-13(15)	380	1	2	3	21,000	6.52	34.31	86.99	3.73	8.38	
$ZnZrO_x$/H-SSZ-13(30)	380	1	2	3	21,000	6.30	35.92	82.58	3.34	7.50	

Supplementary References

1. J. Wang, G. Li, Z. Li, C. Tang, Z. Feng, H. An, H. Liu, T. Liu and C. Li, Sci. Adv., 2017, 3, e1701290.
2. S. Wang, L. Zhang, P. Wang, X. Liu, Y. Chen, Z. Qin, M. Dong, J. Wang, L. He, U. Olsbye and W. Fan, Chem, 2022, 8, 1376-1394.
3. S. Wang, L. Zhang, W. Zhang, P. Wang, Z. Qin, W. Yan, M. Dong, J. Li, J. Wang, L. He, U. Olsbys and W. Fan, Chem, 2020, 6, 3344–3363.
4. S. Wang, L. Zhang, P. Wang, W. Jiao, Z. Qin, M. Dong, J. Wang, U. Olsbye and W. Fan, Nat. Catal., 2022, 5, 1038-1050.
5. J. R. Di Iorio, S. Li, C. B. Jones, C. T. Nimlos, Y. Wang, E. Kunkes, V. Vattipalli, S. Prasad, A. Moini, W. F. Schneider and R. Gounder, J. Am. Chem. Soc., 2020, 142, 4807–4819.
6. J. Zhu, Z. Liu, K. Iyoki, C. Anand, K. Yoshida, Y. Sasaki, S. Sukenaga, M. Ando, H. Shibata, T. Okubo and T. Wakihara, Chem. Commun., 2017, 53, 6796-6799.
7. T. Chatelain, J. Patarin, R. Farré, O. Pétigny and P. Schulz, Zeolites, 1996, 17, 328-333.
8. D. Jo, T. Ryu, G. T. Park, P. S. Kim, C. H. Kim, I. S. Nam and S. B. Hong, ACS Catal., 2016, 6, 2443-2447.
9. Q. Ke, T. Sun, X. Wei, Y. Guo, S. Xu and S. Wang, Chem. Eng. J., 2019, 359, 344-353.
10. X. Liu, M. Wang, C. Zhou, W. Zhou, K. Cheng, J. Kang, Q. Zhang, W. Deng and Y. Wang, Chem. Commun., 2017, 54, 140-143.
11. S. Wang, L. Zhang, W. Zhang, P. Wang, Z. Qin, W. Yan, M. Dong, J. Li, J. Wang, L. He, U. Olsbys and W. Fan, Chem, 2020, 6, 3344–3363.
12. Z. Li, J. Wang, Y. Qu, H. Liu, C. Tang, S. Miao, Z. Feng, H. An and C. Li, ACS Catal., 2017, 7, 544−8548.
13. P. Zhang, L. Ma, F. Meng, L. Wang, R. Zhang, G. Yang and Z. Li, Appl. Catal., B, 2022, 305, 121042.

14. P. Gao, S. Dang, S. Li, X. Bu, M. Qiu, C. Yang, H. Wang, L. Zhong, Y. Han, Q. Liu, W. Wei and Y. Sun, ACS Catal., 2018, 8, 571-578.
15. X. Wang, T. Zeng, X. Guo, Z. Yan, H. Ban, R. Yao, C. Li, X. Gu and M. Yue, Proc. Natl. Acad. Sci., 2024, 121, e2408297121.
16. X. Liu, M. Wang, H. Yin, J. Hu, K. Cheng, J. Kang, Q. Zhang and Y. Wang, ACS Catal., 2020, 10, 8303−8314.